Electronic Supplementary Material (ESI) for Chemical Communications.

Electronic Supplementary Information

Engineering the Surface Chemistry of Lead Chalcogenide Nanocrystal Solids to Enhance Carrier Mobility and Lifetime in Optoelectronic Devices

S. J. Oh, D. B. Straus, T. Zhao J. –H. Choi, S.-W. Lee, E. A. Gaulding, C. B. Murray, and C. R. Kagan*

NC Synthesis

We synthesize 3 nm and 6 nm oleic-acid capped PbSe NCs and 4 nm oleic-acid capped PbS NCs with the first excitonic peak at 1000 nm, 1800 nm and 1100 nm, respectively, following previously reported methods.[1,2] NCs are synthesized under nitrogen atmosphere using air-free Schlenk line procedures.

For 6 nm PbSe NCs, a solution of 892 mg of lead oxide (PbO), 3 mL of oleic-acid, and 20 mL of octadecene (ODE) is heated to 120 °C, degassed for 3 h under vacuum and heated to 180 °C. The Se precursor (1M Trioctylphosphine:Se and 60 μL of Diphenylphosphine) is quickly injected. After a 100 s reaction time, the solution is quenched by a water bath to room temperature. 2 mL of hexane and 20 mL of ethanol are added to the solution, and the solutions are precipitated by centrifuging at 10,000 rpm for 2 min, and redispersed in 5 mL of hexane. The washing process is repeated three times. Finally, NCs are redispersed in octane solution and stored in a nitrogen glovebox.

For 3 nm PbSe NCs, a solution of 446 mg of PbO, 1.55 mL of oleic-acid, and 25 mL of ODE is heated to 120 °C, degassed for 3 h under vacuum and heated to 140 °C. The Se precursor (bis-(trimethylsilyl) selenide in 8 mL ODE / Note: Bis(trimethylsilyl) selenide is toxic by vapor inhalation and skin absorption) is rapidly injected into the solution. After a 80-150 s reaction time, the solution is quenched to room temperature using a water bath. The NCs are similarly purified with hexane, ethanol, and acetone three times, and finally redispersed in octane solution and stored in a nitrogen glovebox.

For 4 nm PbS NCs, 0.47g of PbO, 23 mL of ODE and 2 mL of oleic-acid are degassed in a three-neck flask at 120 °C for 2 h under vacuum and then the environment is switched to N_2. Bis-(trimethylsilyl) sulfide is mixed with ODE (21 μL./mL) inside the glovebox and taken out to inject into the reaction flask swiftly. The heating mantle is turned off and removed 20 s after the injection. A water bath is used to cool down the reaction flask. The NC dispersion is transferred into the glovebox without air exposure and purified by washing with acetone and 2-propanol 3 times. The final NC product is dispersed in octane/hexane (4:1) at desired concentrations.

NC thin film deposition and ligand exchange

Lead chalcogenide NC thin films are deposited by spin coating to form NC thin films on different substrates for chemical, structural, optical and electronic characterization. Quartz is used as a substrate for absorption characterization, or to produce photoconductor-based photodetector devices; double-polished silicon wafers are used as substrates for Fourier transmission infrared (FTIR) spectroscopy; thermally-oxidized silicon wafers are used as substrates for FET devices; and Corning Eagle 2000 glass pieces are used as substrates for time-resolved microwave conductivity (TRMC) measurements. Substrates are washed with acetone, iso-propanol, and deionized water, exposed to UV-ozone for 30 min, and then treated with mercaptopropyltrimethoxysilane (MPTS) to improve the adhesion of the NCs to the substrate surfaces.[3,4] The oleic-acid capped NC thin-film samples are treated by immersion in 30 mM solutions of NH_4SCN in methanol or 1 mM solutions of BDT in acetonitrile for 1 min and are washed in the parent solvent three times.

FET Device Fabrication

Heavily p-doped Si wafers with 250 nm of SiO_2 are used as substrates, which serve as back gate and part of dielectric layer, respectively. A 20 nm $Al2O_3$ layer is deposited to complete the dielectric layer by atomic layer deposition. The substrates are treated with MPTS and NC thin films are formed, as describe in the previous section. Au (30nm) source and drain electrodes are deposited by evaporation through a shadow mask to define channel lengths of 200 µm and widths of 3000 µm.

TRMC Characterization

TRMC measurements, X-band microwaves are generated by an HP 83712A synthesized CW generator coupled to an isolator (Pasternack) to prevent back-reflection into the source. The microwaves then pass through a circulator into a WR90 microwave antenna (Penn Engineering) that is connected to a home-built resonant cavity designed to have a resonance peak near 9 GHz when loaded with a thin-film sample deposited on a 1.1 mm thick Corning Eagle 2000 glass substrate. Samples are loaded into the air-tight resonant cavity in a nitrogen filled glove box. 3-5 ns pulses of 532 nm light are produced by a Continuum Minilite II Nd:YAG laser and are focused through a sealed aperture in the resonant cavity, expanding to a spot size of approximately 9 mm. Microwaves couple out of the resonant cavity and are directed by the circulator into a Faraday cage, and then pass through a Minicircuits VHF-7150+ high pass filter before being directed to a microwave switch (Minicircuits USB-8SPDT-A18). The resonance peak is found using an HP 8566B spectrum analyzer, and once tuned to the resonance frequency of the loaded resonant cavity, microwaves are directed to a Keysight 8472B microwave detector to convert microwave power to DC voltage and amplified 25 times by an impedance matching amplifier (Comlinear CLC-221). The reflected power in the absence of light is measured on our Keysight DSO-S 054A oscilloscope, and TRMC transients are high-pass filtered and further amplified 100 times by an HP 462A amplifier before being detected.

The theory of TRMC is described in detail elsewhere.[5,6] We signal process our data by low-pass filtering using a Butterworth filter of the fifth order with a 30 MHz cutoff frequency and use deconvolution to remove the cavity response using the known response function of our resonant cavity.[7] We are assuming the dielectric constant of the cavity is constant. TRMC transients for PbSe and PbS NC thin films are fit to the sum of two exponentials, and fit parameters are detailed in Table II.

FET, solar cell, and photoconductor Characterization

The FET devices are characterized using an Agilent 4156C semiconductor parameter analyzer combined with a Karl Suss PM5 probe station in the nitrogen glove box. The solar cell devices are sealed in a cell with a nitrogen atmosphere and their characteristics are measured using a Keithley 2400 sourcemeter under the illumination of AM 1.5G solar simulated light (1 Sun, Oriel 96000 Newport). The photoconductor devices are similarly sealed in a nitrogen atmosphere and their characteristics are measured with an Agilent 4156C semiconductor parameter analyzer or Keithley 2400 sourcemeter under the illumination of 488 nm light from a Coherent Innova Ar:Kr laser.

Discussions on conductivity

The two-terminal conductivity of BDT-treated thin films is 6.2×10^{-6} S/cm and that of SCN-treated thin films is 3.1×10^{-3} S/cm (Fig. S1, ESI). In comparison to BDT-treated NC thin films, the 500 times higher conductivity of SCN-treated NC samples is dominated by its 100 times higher carrier mobility, consistent with the reduction or even elimination of the interparticle spacing (Fig. 2A,B), and suggests a 5 times higher hole carrier concentration. As the mobility is measured under an applied gate bias while the conductivity is not, the carrier concentration cannot be calculated quantitatively. Higher hole concentrations are consistent with previous reports of higher levels of oxygen doping in SCN-treated PbSe NC thin films, as SCN more sparsely covers the NC surface.

Discussions on NC thin film FETs, solar cells, and photoconductors

While we use 1800 nm PbSe NCs in FETs because larger NCs show the highest carrier mobilities,[8] we choose 1100 nm PbS NCs and 1000 nm PbSe NCs from which to fabricate Schottky solar cells, as small PbS and PbSe NCs are well-matched to the solar spectrum and are known to form high efficiency solar cells.[9] While more insulating, small PbS NC thin films used for photovoltaic cells are difficult to characterize using FET measurements, we confirm that n-type behavior of lead deposited NC thin films and p-type behaviour of tetramethylammonium hydroxide treated NC thin films is achieved using these treatments on analogous PbSe NC thin film FETs [Fig. S5, ESI]. We also fabricate PbS NC thin film photodetectors using hybrid ligand exchange that shows stable photoconductive response and fast switching behaviour, consistent with the lower activity of the sulphide toward oxygen [ESI S3 (A)].[10]

Discussions on NC devices measured with different techniques.

We note differences in FET, photoconductor, and TRMC measurements; such as the gate field in the FET, device interface effects at the gate insulator and electrical contacts in the FET and the photoconductor, and the time- and length-scale of TRMC; influence the values found for carrier mobility and lifetime and their quantitative representation of materials properties. However, all measurements show that our hybrid ligand treatment enhances the NC thin film mobility-lifetime product

Table I. Majority carrier hole characteristics of PbSe NC thin films treated with BDT, SCN, and SCN followed by BDT. Reported uncertainties are one standard deviation.

	Field Effect Mobility [cm^2/Vs]	I_{PH} at 10V [A]	I_{PH}/ I_{DARK}	Normalized Lifetime	Normalized mobility-lifetime product
BDT	9.10 (±2.50) x 10^{-4}	1.85 (±0.08) x 10^{-8}	7.71(±0.4)	1.00	1.00
SCN	9.40 (±3.50) x 10^{-2}	3.50 (±0.14) x 10^{-8}	0.15(±0.01)	0.0183	1.89
SCN-BDT	2.90 (±0.70) x 10^{-1}	5.28(±0.22) x 10^{-6}	3.62(±0.2)	0.896	285

Table II: Fit parameters for TRMC transients. The transients are fit to the function $\phi\Sigma\mu(t) = A_1\exp\left(-\frac{t}{t_1}\right) + A_2\exp\left(-\frac{t}{t_2}\right)$. The fit parameters $f_1 = A_1/(A_1 + A_2)$ and $f_2 = A_2/(A_1 + A_2)$. The lifetime is $f_1 t_1 + f_2 t_2$. Uncertainties are standard errors of the mean. PbE (E=S, Se)_NC thin film mobility-quantum yield products and mobility-lifetime products are normalized by the mobility-quantum yield products and mobility-lifetime products of PbE NC thin films treated with BDT.

Sample	Normalized Mobility-QY Product (a.u.)	Lifetime (µs)	f_1	t_1 (µs)	f_2	t_2 (µs)	Normalized Mobility-Lifetime Product (a.u.)
PbSe BDT	1.0 ± 0.1	6 ± 2	0.5 ± 0.1	0.5 ± 0.1	0.50 ± 0.09	12 ± 2	1.0 ± 0.3
PbSe SCN	159 ± 7	0.116 ± 0.008	0.92 ± 0.06	0.050 ± 0.001	0.076 ± 0.006	0.92 ± 0.05	2.9 ± 0.2
PbSe SCN + BDT	147 ± 5	0.24 ± 0.01	0.90 ± 0.06	0.73 ± 0.04	0.105 ± 0.005	1.68 ± 0.09	5.6 ± 0.4
PbS BDT	1.00 ± 0.09	2.3 ± 0.4	0.63 ± 0.09	0.34 ± 0.05	0.37 ± 0.06	5.6 ± 0.8	1.0 ± 0.2
PbS SCN	16 ± 1	2.9 ± 0.3	0.44 ± 0.08	0.53 ± 0.06	0.56 ± 0.05	4.7 ± 0.5	21 ± 3
PbS SCN + BDT	19.7 ± 0.9	3.8 ± 0.4	0.46 ± 0.03	0.67 ± 0.08	0.54 ± 0.04	6.4 ± 0.5	33 ± 3

Table III. The photoconductor performance of PbSe NC thin films treated with BDT, SCN, and SCN followed by BDT. (Note : The device area is 2.4 x 10^{-4} cm^2, and the excitation wavelength is 488 nm. The absorbance around 488 nm is higher than 0.6, as seen in Supporting Information Figure S5 (B), corresponding to absorption around 75% in the NC thin films. We assume 100% light absorption, which will underestimate the gain, so the calculated gain is a lower limit.

	I_{PH} at 20V [A]	Current Density [Acm^{-2}]	Laser Power Density [W cm^{-2}]	Responsivity [A W^{-1}]	Number of electrons per unit area per second [cm^{-2}s^{-1}]	Number of photons per unit area per seconds [cm^{-2}s^{-1}]	Gain
BDT	3.7 x 10^{-8}	1.54 x 10^{-4}	2.63 x 10^{-4}	0.59	9.62 x 10^{14}	6.46 x 10^{14}	1.49
SCN	7.01 x 10^{-8}	2.92 x 10^{-4}	2.63 x 10^{-4}	1.11	1.82 x 10^{15}	6.46 x 10^{14}	2.82
SCNBDT	1.06 x 10^{-5}	4.40 x 10^{-2}	2.63 x 10^{-4}	167	2.75 x 10^{17}	6.46 x 10^{14}	425

Table IV The photovoltaic performance of PbS NC solar cells with only BDT treatment and the hybrid SCN- and BDT-treatment.

	JSC [mA/cm2]	VOC [V]	FF	PCE [%]
PbS NC solar cell with BDT treatment	12.4	0.407	0.41	2.1
PbS NC solar cell with hybrid treatment	14.4	0.432	0.56	3.5

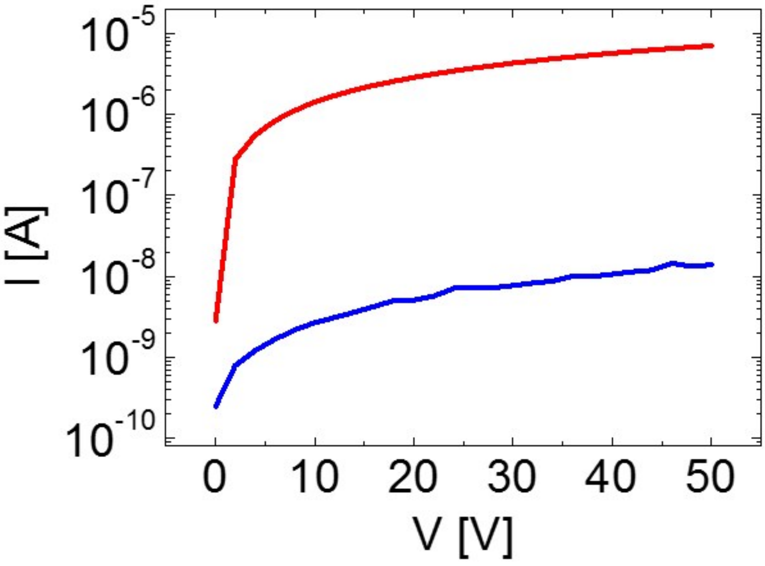

Figure S1. Two-terminal I-V characteristics of PbSe NC thin films treated with (blue) BDT and (red) SCN used to calculate film conductivity.

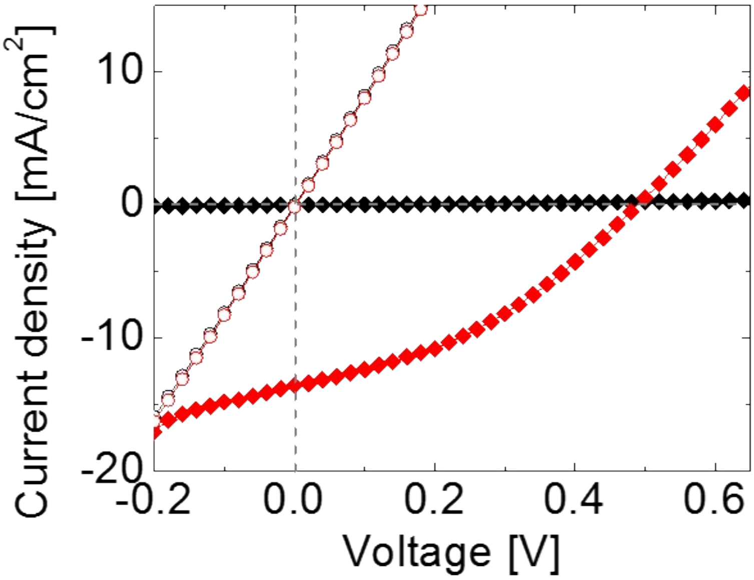

Figure S2. I-V curves of PbSe NC thin-film Schottky solar cells in which the NCs are treated with (closed diamond) BDT and (open circle) SCN and the cells are measured (black) in the dark and (red) under illumination.

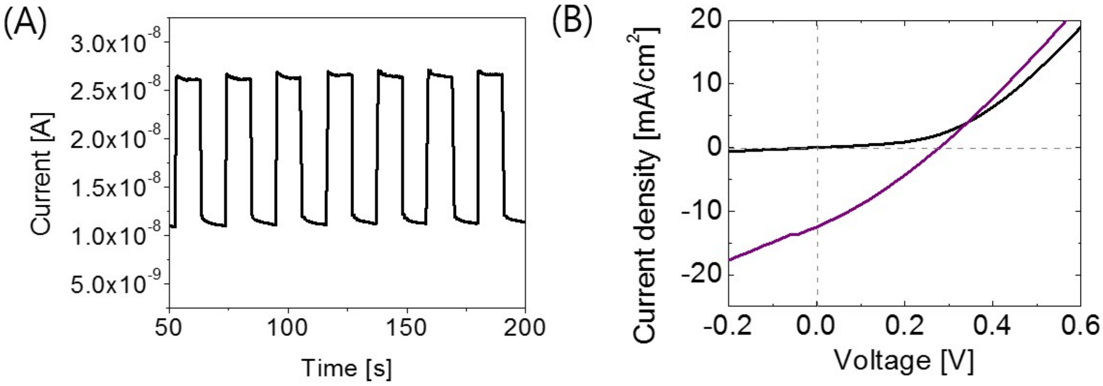

Figure S3. (A) Photocurrent response for periodic 488 nm excitation of PbS NC thin films treated using the hybrid ligand exchange process. (B) I-V curves of PbS NC thin-film Schottky solar cells treated using the hybrid, SCN and BDT ligand exchange process (black) in the dark (purple) and under illumination.

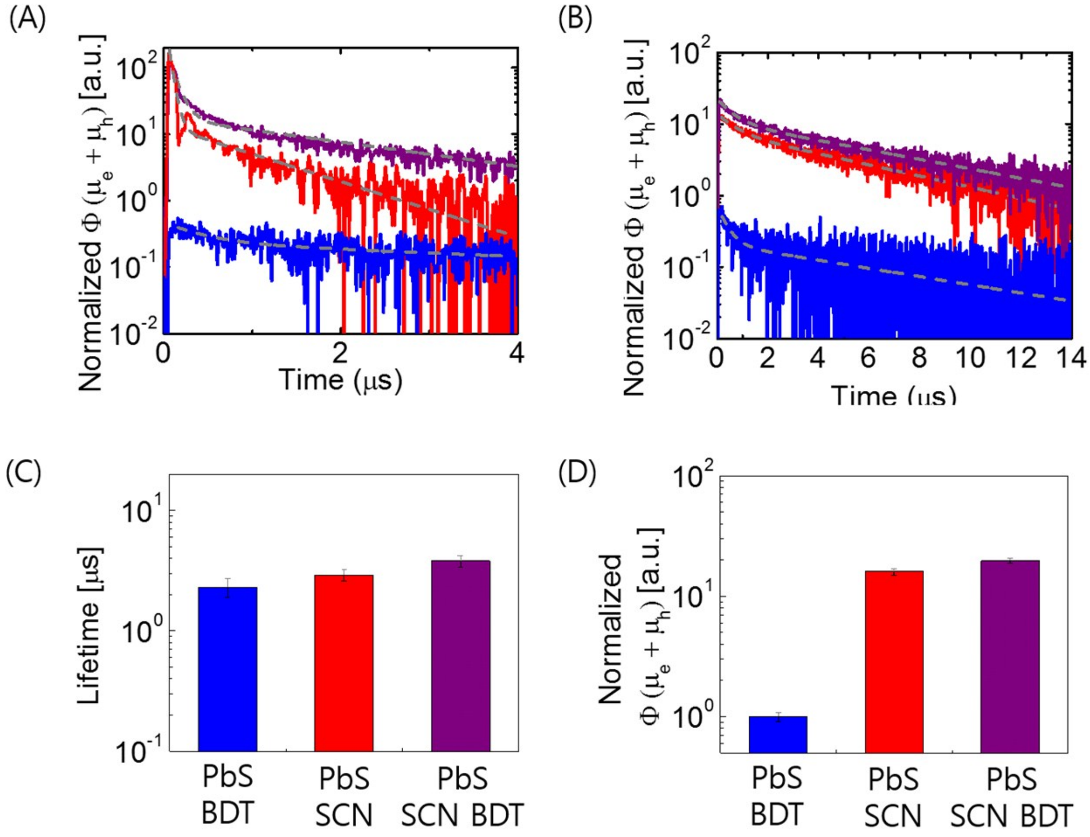

Figure S4. Representative TRMC mobility-quantum yield product transients for (A) PbSe NC thin films and (B) PbS NC thin films treated with (blue) BDT, (red) SCN, and (purple) SCN followed by BDT. PbE (E=S, Se)_NC thin film mobility-quantum yield products are normalized by the average mobility-quantum yield products of PbE NC thin films treated with BDT. (C) Lifetime of and (D) quantum yield-mobility product of PbS NC thin films treated with (blue) BDT, (red) SCN, and (purple) SCN followed by BDT.

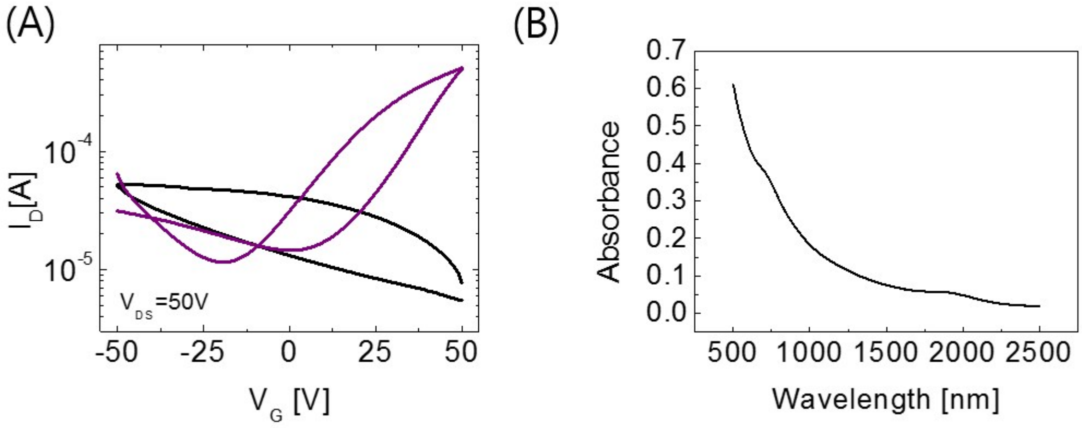

Figure S5. (A) Transfer curves of 6 nm PbSe NC thin-film FETs treated with (black) TMAOH and (purple) hybrid ligand treatment of SCN and BDT followed by 1 nm lead deposition. (B) Absorption spectrum of PbSe NC thin films treated with SCN followed by BDT.

References

1 S. J. Oh, N. E. Berry, J.-H. Choi, E. A. Gaulding, T. Paik, S.-H. Hong, C. B. Murray and C. R. Kagan, *ACS Nano*, 2013, **7**, 2413–2421.

2 W. W. Yu, J. C. Falkner, B. S. Shih and V. L. Colvin, *Chem. Mater.*, 2004, **35**, 3318–3322.

3 S. J. Oh, N. E. Berry, J.-H. Choi, E. A. Gaulding, H. Lin, T. Paik, B. T. Diroll, S. Muramoto, C. B. Murray and C. R. Kagan, *Nano Lett.*, 2014, **14**, 1559-1566

4 S. J. Oh, Z. Wang, N. Berry, J.-H. Choi, T. Zhao, E. A. Gaulding, T. Paik, Y. Lai, C. B. Murray, and C. R. Kagan *Nano Lett.*, 2014, **14**, 6210-6216.

5 P. P. Infelta, M. P. De Haas and J. M. Warman, *Radiat. Phys. Chem.*, 1977, **10**, 353–365.

6 T. J. Savenije, A. J. Ferguson, N. Kopidakis and G. Rumbles, *J. Phys. Chem. C*, 2013, **117**, 24085–24103.

7 D. B. Straus, E. D. Goodwin, E. A. Gaulding, S. Muramoto, C. B. Murray and C. R. Kagan, *J. Phys. Chem. Lett.*, 2015, **6**, 4605–4609.

8 Y. Liu, M. Gibbs, J. Puthussery, S. Gaik, R. Ihly, H. W. Hillhouse and M. Law, *Nano lett.*, 2010, **10**, 1960–1969.

9 A. H. Ip, S. M. Thon, S. Hoogland, O. Voznyy, D. Zhitomirsky, R. Debnath, L. Levina, L. R. Rollny, G. H. Carey, A. Fischer, K. W. Kemp, I. J. Kramer, Z. Ning, A. J. Labelle, K. W. Chou, A. Amassian and E. H. Sargent, *Nat. Nanotechnol.*, 2012, **7**, 577–582.

10 J. Zhang, J. Gao, C. P. Church, E. M. Miller, J. M. Luther, V. I. Klimov and M. C. Beard, *Nano Lett.*, 2014, 14, 6010-6015